Characterization of near-wall accumulation regions for inertial particles in turbulent boundary layers

Maurizio Picciotto, Cristian Marchioli, and Alfredo Soldati[a)]
Centro Interdipartimentale di Fluidodinamica e Idraulica, Dipartimento di Energetica e Macchine, Università degli Studi di Udine, Via delle Scienze 208, 33100 Udine, Italy

(Received 2 March 2005; accepted 30 June 2005; published online 12 September 2005)

In this paper, we examine particle distribution in the wall region of turbulent boundary layers, considering specific flow conditions ($\mathrm{Re}_\tau = 150$) and spanning two orders of magnitude of particle inertial parameter—the particle timescale. First, we identify the flow timescales that govern particle distribution, examining the degree of particle preferential concentration and determining the optimum in connection with particle timescale. Second, we identify which of the flow variables may be used to control particle distribution. These are the streamwise and spanwise shear stress components at the wall, which correspond to the only nonvanishing elements of the fluctuating fluid velocity gradient tensor. © *2005 American Institute of Physics*. [DOI: 10.1063/1.2033573]

Controlling particle distribution in turbulent flow near a wall could improve the efficiency of heat, mass, and momentum transfer processes in a number of industrial and environmental applications, such as multiphase flow reactors and combustion or post-combustion devices. As shown by several experiments[1,2] and numerical simulations,[3–5] particle distribution in turbulent shear flows is known to be highly inhomogeneous due to the action of near-wall coherent flow structures. These structures are responsible for particle accumulation and segregation into elongated clusters, which correlate well with the instantaneous position of the low-speed streaks at the wall.[1,2] Based on this observation, particle distribution control may be achieved by boundary layer manipulation. A possible strategy is to treat the turbulent boundary layer as a black box and to observe the structural changes when the boundary conditions are modified. Looking at boundary layers in this fashion is certainly a way forward. Still, current literature lacks objective criteria for particle accumulation, which should go beyond observing long-term particle clustering along low-speed streaks.[1–5] We thus need to define clearly and in a quantitative way which of the flow variables is best suited for devising feasible flow-control strategies. This is the final aim of our research.

In this work, we focus precisely on the wall region ($z^+ < 5$ in nondimensional units along the wall-normal direction), where the flow is depleted from strongly coherent structures yet it is complicated enough to induce particle-selective distribution.[1–5] Rouson and Eaton[6] (R&E hereinafter) investigated particle distribution in connection with the flow topology classification based on the invariants of the velocity gradient tensor.[7] R&E[6,8] found that moderate- to high-inertia particles in turbulent channel flow sample preferentially convergence rather than vortical-flow regions. Different from these previous works in channel flow,[6,8] we consider a range of particle parameters matching the timescale range of the fluid structures in the wall region. First, we will examine the relationship between convergence-flow regions and particle instantaneous location in the viscous sublayer. Second, we will try to establish a connection between convergence regions and regions of particle accumulation. Specifically, we will discriminate between regions of short- and long-term accumulation using threshold values of the wall shear stress components, which in turn correspond to the only nonvanishing elements of the fluctuating velocity gradient tensor computed at the wall.

We used pseudospectral direct numerical simulation[9] to compute the turbulent Poiseuille flow of air (incompressible and Newtonian) in a two-dimensional channel at $\mathrm{Re}_\tau = u_\tau h/\nu = 150$, where u_τ is the friction velocity,[10] ν is fluid viscosity, and h is the channel half-height. The reference geometry consists of two infinite, vertical, flat, parallel walls with periodic boundary conditions in the streamwise (x) and spanwise (y) directions and no-slip conditions at the walls. The computational domain is $1885 \times 942 \times 300$ wall units (i.e., in terms of variables identified with the superscript "+" made dimensionless using ν and u_τ) in x, y, and z, discretized with $128 \times 128 \times 129$ grid nodes.

We tracked four swarms—$O(10^5)$—of particles, characterized by values of the Stokes number St equal to 1, 5, 25, and 125. In wall turbulence, the Stokes number may be expressed as particle time scale, $\tau_p = \rho_p d_p^2/18\mu$, made dimensionless using ν and u_τ. Since we are currently interested in characterizing the collective behavior of particles, we chose a simplified numerical setting in which particle number density and particle size are small enough to neglect feedback onto the gas flow (one-way coupling approach). In our simulations, particles are pointwise, rigid, elastically rebounding spheres. The Lagrangian equation of particle motion includes only the effects of particle inertia and nonlinear Stokes drag. Initially, particle number concentration is uniform in the computational box and particle position is chosen randomly.

R&E[6] examined the tendency of inertial particles to sample preferentially the non-homogeneous turbulent flow field of a two-dimensional channel using the topological

[a)]Author to whom correspondence should be addressed. Also affiliated with Department of Fluid Mechanics, CISM, 33100 Udine, Italy. Electronic mail: soldati@uniud.it

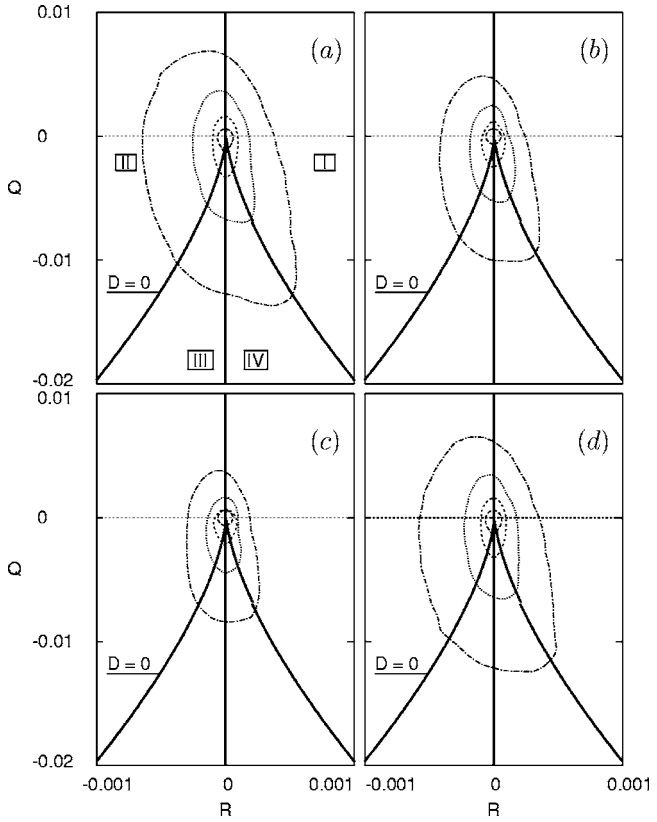

FIG. 1. Viscous sublayer ($z^+<5$) joint PDF of Q, R conditionally sampled at St=1 (a), St=5 (b), St=25 (c), and St=125 (d) particle positions, respectively. Isoline values are –– PDF=10, --- PDF=1, ··· PDF=0.1, and –·– PDF=0.01.

classification scheme by Chong *et al.*[7] R&E[6] tracked ensembles of moderate- to high-Stokes number particles (St=8.6, 117, and 810) throughout the entire channel. This range includes particles too big to match the ever-decreasing turbulent flow scales, which particles encounter when approaching the wall. Our first object here is to use the same methodology of R&E[6] extending the analysis to low-to moderate-Stokes number particles, which are more "respondent" to the near-wall flow timescales.

The topological classification scheme[7] is based on the invariants of the velocity gradient tensor $u_{i,j}$: $P=u_{i,i}$, $Q=[(u_{i,i})^2-u_{i,j}u_{j,i}]/2$, and $R=\det[u_{i,j}]$. For incompressible flow fields (as in the present case), $P=0$ and all flow topologies can be classified in the (Q,R) plane.[7]

We thus computed Q and R for the fluid at each grid point in the viscous sublayer ($z^+<5$); then, we sampled conditionally Q and R at particle position.[6] Figure 1 shows four decades of the resulting joint probability density function (PDF) for particles and demonstrates their preference for or against any of the instantaneous flow topology in the (Q,R) plane.[6] In Fig. 1(a), four regions can be identified: two vortical-flow regions—the stable focus/stretching (*I*) and unstable focus/compressing critical nodes (*II*)—and two convergence regions—the stable node/saddle/saddle (*III*) and unstable node/saddle/saddle critical nodes (*IV*).

Also for the currently investigated particle sizes, the most probable value of Q and R is zero for all the instantaneous realizations studied.[6] The PDF sampled at the position of St=1 particles, shown in Fig. 1(a), is similar to that of the fluid (not shown) and indicates weak preferential sampling: the preferred topologies correspond to quadrants *II* and *IV*. The degree of particle preferential sampling increases monotonically for the intermediate-size particles: the area covered in the (Q,R) plane by the PDFs shown in Fig. 1(b) for St=5 particles and in Fig. 1(c) for St=25 particles becomes smaller, indicating that these particles avoid the strongest vortical regions in the first two topological quadrants as well as the strongest vortex-stretching regions along the positive-R, zero-D line. A broader PDF approaching the St=1 particle curves is obtained for St=125 particles, as shown in Fig. 1(d). This indicates a less pronounced preferential sampling by the larger particles.

TABLE I. Percent particle number density in the topological quadrants according to the classification scheme by Chong *et al.* (Ref. 7).

Topol. Quadrant	Topological Region	St=1 (%)	St=5 (%)	St=25 (%)	St=125 (%)
I	Vortical	11.1	10.4	10.5	11.5
II	Vortical	16.5	14.7	14.4	16.5
III	Convergence	34.0	36.2	36.4	34.0
IV	Convergence	38.4	38.7	38.7	38.0

A quantitative clearcut analysis including the influence of particle inertia is made difficult by the massive clustering of points around the origin. Thus, in Table I we report the results from percent particle counts for each topological quadrant and for each particle set. A larger proportion of particles tends to occupy the convergence regions (topological quadrants *III* and *IV*), while the strongest vortical regions (topological quadrants *I* and *II*) are depleted of particles due to the centrifuge-like effect of the eddies in the near-wall region.[6] This further confirms that particles in the viscous sublayer concentrate preferentially in convergence-flow regions and that this tendency depends on the particle-to-fluid timescale ratio, namely, the particle Stokes number. As suggested by a similar analysis in different flow configurations, particle concentration in specific flow regions is observed when the flow structure timescale and the particle timescale are comparable. In the present study, the maximum preferential concentration is found for the intermediate-size particles ($St\simeq 25$). This maximum may be demonstrated using an integral parameter as shown in Fig. 2, where we plot the maximum deviation from randomness, $D_{\max}$, calculated as $(\sigma-\sigma_{\text{Poisson}})/m$, where σ and σ_{Poisson} represent respectively the standard deviations for the particle number density distribution and the Poisson distribution ($t^+=6500, z^+<5$) and m is the mean particle number density.[6,8,11] This indicates that particle dynamics in the viscous sublayer is controlled by flow structures with timescale τ_f around 25. Considering that τ_f scales linearly with wall distance and decreases progressively as the turbulence structures lie closer to the wall, we can infer that these timescales correspond to the circulation time of the turbulence structures in the buffer layer ($5<z^+<30$).[12]

In a recent work, Chacin and Cantwell[13] showed that

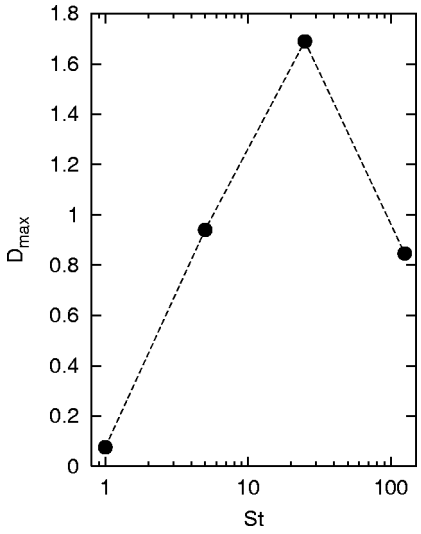

FIG. 2. Deviation from randomness, D_{max}, as a function of the particle Stokes number $St(t^+=6500, z^+<5)$. $D_{max}=(\sigma-\sigma_{Poisson})/m$; σ is the standard deviation of the particle number density distribution; $\sigma_{Poisson}$ is the standard deviation of the Poisson distribution; and m is the mean particle number density.

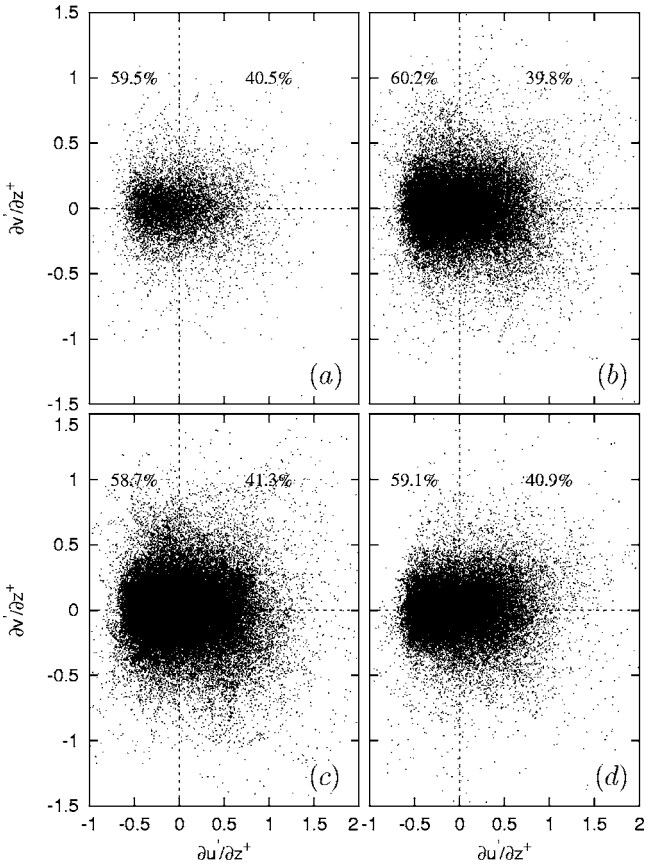

FIG. 3. Viscous sublayer ($z^+<5$) probability distribution functions of nonvanishing components of the fluctuating strain tensor, conditionally sampled at St=1 (a), St=5 (b), St=25 (c), and St=125 (d) particle positions, respectively.

convergence-flow regions generated in the viscous sublayer by near-wall sweeps, which in turn feed the high-speed regions, can be characterized using Q and R and belong to the *IV* topological quadrant. Their analysis showed also that ejection-like near-wall regions, which characterize the activity of the low-speed streaks and are also convergence-flow regions, do not possess clearcut classification in the (Q,R) plane so that it is difficult to pinpoint their quadrant of pertinence. This has to do with the scarce influence of the ejections in the viscous sublayer, which is dominated by the sweep activity.[14] In a previous work,[5] we observed the following cycle of particle deposition and resuspension or segregation: particles are entrained by the sweeps, reach (not necessarily touch) the wall in correspondence of the high-speed regions, and move towards the low-speed streaks, where they tend to remain for long times.[15] As discussed before,[13] we cannot rely only on the analysis in the (Q,R) space to discriminate between convergence long- and short-term accumulation regions, but we need a further set of criteria specifically valid in the wall proximity.

We observe that near-wall flow regions can be identified with respect to the wall-normal direction in terms of the shear stress: sweep-generated, high-speed regions are characterized by $\tau'_{xz}|_w>0$ associated to $\tau'_{yz}|_w\simeq 0$, whereas ejection-like, low-speed regions are characterized by $\tau'_{xz}|_w<0$ associated to $\tau'_{yz}|_w\simeq 0$. Here, $\tau'_{xz}|_w$ and $\tau'_{yz}|_w$ are the streamwise and spanwise fluctuating components of the wall shear stress and correspond precisely to $\partial u'/\partial z|_w$ and $\partial v'/\partial z|_w$, which are the only nonvanishing elements of the fluctuating part of the velocity gradient tensor, $u'_{i,j}$, evaluated at the wall.

We computed $\partial u'/\partial z|_w$ and $\partial v'/\partial z|_w$ for each particle set (sampled at particle position). First, particle location in the viscous sublayer ($z^+<5$) was identified and projected onto the wall; then, the components of $u'_{i,j}$ at the projected wall location were computed. The resulting scatter plots in the $(\partial u'/\partial z|_w, \partial v'/\partial z|_w)$ plane are shown in Fig. 3: visual inspection indicates that particles accumulate preferentially in wall regions characterized by negative values of $\partial u'/\partial z|_w$, i.e., by negative values of $\tau'_{xz}|_w$. To have quantitative data, we counted the sample points falling in each $\partial u'/\partial z|_w$ semiplane. Percent figures for particles have been included in Fig. 3 and confirm that, depending on particle inertia, persistent clusters within the viscous sublayer sample preferentially the negative $\partial u'/\partial z|_w$ semiplane, which corresponds to ejection-like low-speed regions. For comparison purposes, percent figures for the fluid (sampled at grid points) were also computed. We found that 56.5% of the fluid samples fall in the $\partial u'/\partial z|_w<0$ semiplane and only 43.5% in the $\partial u'/\partial z|_w>0$ semiplane. This preferential distribution can be explained considering that grid points sample low-speed regions (in which $\partial u'/\partial z^+|_w<0$) more often than high-speed regions (in which $\partial u'/\partial z^+|_w>0$). This is due to the different spatial extension of sweeps compared to ejections which, we remark, are the mechanisms feeding the low- and high-speed wall regions, respectively. We also counted samples falling in each $\partial v'/\partial z|_w$ semiplane. Percent data (not shown) indicate that the near-wall flow regions correlate well with values of $\partial v'/\partial z|_w$ close to zero.

To clarify some aspects of the above observations, we examined a large number of snapshots showing particle distribution inside the viscous sublayer ($z^+<5$) in connection

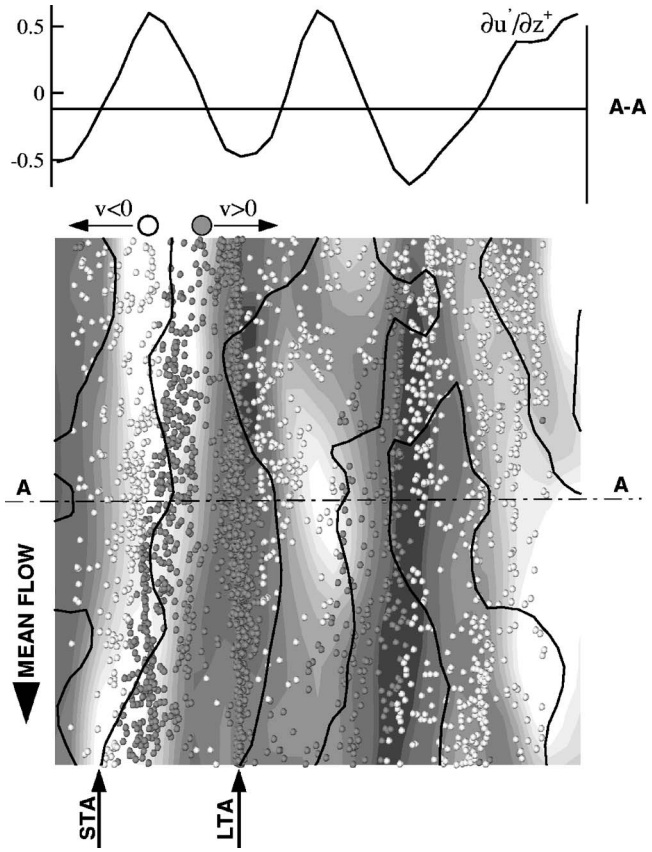

FIG. 4. Instantaneous St=25 particle distribution in the viscous sublayer ($t^+=6500, z^+<5$). The mean flow is directed top down.

with the shear stress distribution at the wall. In Fig. 4, we show a computational window 400 wall units long and 250 wall units wide in the (x,y) plane, sketching the instantaneous distribution of the St=25 particles, chosen for their relatively larger tendency to preferential sampling, together with the contours of the streamwise fluctuating component of the wall shear stress, $\tau'_{xz}|_w = \mu \partial u'/\partial z^+|_w$. The behavior of $\partial u'/\partial z^+|_w$ along the spanwise direction at a fixed streamwise location ($x^+=200$ identified with the dash-dotted *AA* line) is also shown on top of Fig. 4. The gray scales for particles and shear stress are as follows: Dark gray spheres represent particles with positive spanwise velocity ($v>0$), moving from left to right; light gray spheres represent particles with negative spanwise velocity ($v<0$), moving from right to left. Dark gray contours indicate high positive values of $\partial u'/\partial z^+|_w$, white contours indicate low negative values. To complete the picture, black solid lines connect points where $\tau'_{yz}|_w = \mu \partial v'/\partial z|_w$ is equal to zero. From Fig. 4, it is apparent that particles arriving at the wall are initially found in high-speed, high-shear regions (white contours), which are convergence-flow regions where $\partial u'/\partial z|_w$ attains a local maximum. The particles stay briefly in the high-speed regions: they are swept away from these regions and clusters begin to split along the $\partial v'/\partial z|_w=0$ lines, which thus mark the position of short-term accumulation (STA) regions. One of the STA lines is indicated by an arrow on the left side of Fig. 4. The particles move in the spanwise direction toward low-speed, low-shear regions (dark gray contours), where $\partial u'/\partial z|_w$ attains a local minimum, i.e., the low-speed streaks. In these regions, particles line up and form persistent clusters flanking the $\partial v'/\partial z|_w=0$ lines, which now mark the position of long-term accumulation (LTA) regions. One of the LTA lines is indicated by the arrow on the left side of Fig. 4.

Current results can be used to address the problem of imposing particle distribution in turbulent flow near a wall since they add to the physical understanding of particle behavior in the wall region. They incorporate a quantitative criterion for particle wall accumulation to the set identified by R&E[6] based on flow topology classification. This criterion can be of relevance in applications where particle wall distribution control is sought since it connects particle preferential position with threshold values of the components of the wall shear stress which, in turn, is the key variable in boundary layer flow manipulation.[16] Modifications of these components can be easily produced by passive or active devices and should lead to structural changes in particle distribution without the need of capturing the structural details of the coherent structures in turbulent shear flows.

Financial support from MIUR in the frame of the FIRB 2003 program under Grant No. RBAU012FRS_001 and Grant No. RBAU01NZH7_007 is gratefully acknowledged.

[1] D. Kaftori, G. Hetsroni, and S. Banerjee, "Particle behavior in the turbulent boundary layer. II. Velocity and distribution profiles," Phys. Fluids **7**, 1107 (1995).
[2] M. Righetti and G. P. Romano, "Particle-fluid interactions in a plane near-wall turbulent flow," J. Fluid Mech. **505**, 93 (2004).
[3] H. Zhang and G. Ahmadi, "Aerosol particle transport and deposition in vertical and horizontal turbulent duct flows," J. Fluid Mech. **406**, 55 (2000).
[4] L. M. Portela, P. Cota, and R. V. A. Oliemans, "Numerical study of the near-wall behaviour of particles in turbulent pipe flows," Powder Technol. **125**, 149 (2002).
[5] C. Marchioli and A. Soldati, "Mechanisms for particle transfer and segregation in turbulent boundary layer," J. Fluid Mech. **468**, 283 (2002).
[6] D. W. Rouson and J. K. Eaton, "On the preferential concentration of solid particles in turbulent channel flow," J. Fluid Mech. **428**, 149 (2001).
[7] M. S. Chong, A. Perry, and B. J. Cantwell, "A general classification of three-dimensional flow fields," Phys. Fluids A **2**, 765 (1990).
[8] J. K. Eaton and J. R. Fessler, "Preferential concentration of particles by turbulence," Int. J. Multiphase Flow **20**, 169 (1994).
[9] A. Soldati and S. Banerjee, "Turbulence modification by large scale organized electrohydrodynamic flows," Phys. Fluids **10**, 1742 (1998).
[10] The friction velocity is defined as $u_\tau=\sqrt{\tau_w/\rho}$, where τ_w is the wall shear stress and ρ is the fluid density.
[11] Here "random" is defined as the situation in which any given particle is equally likely to appear in any given cell so that one can show that the particle number distribution approaches a Poisson distribution (Ref. 6).
[12] W. Schoppa and F. Hussain, "Coherent structure generation in near-wall turbulence," J. Fluid Mech. **453**, 57 (2002).
[13] J. M. Chacin and B. J. Cantwell, "Dynamics of a low Reynolds number turbulent boundary layer," J. Fluid Mech. **404**, 87 (2000).
[14] W. W. Willmarth and S. S. Lu, "Structure of the Reynolds stress near the wall," J. Fluid Mech. **55**, 65 (1972).
[15] C. Narayanan, D. Lakehal, L. Botto, and A. Soldati, "Mechanisms of particle deposition in a fully-developed turbulent open channel flow," Phys. Fluids **15**, 763 (2003).
[16] J. Kim, "Control of turbulent boundary layers," Phys. Fluids **15**, 1093 (2003).